APL Materials

REVIEW ARTICLE | APRIL 14 2017

Research Update: Nanogenerators for self-powered autonomous wireless sensors

Special Collection: Nanogenerators

Usman Khan; Ronan Hinchet ; Hanjun Ryu; Sang-Woo Kim

APL Mater. 5, 073803 (2017)
https://doi.org/10.1063/1.4979954

APL MATERIALS **5**, 073803 (2017)

Research Update: Nanogenerators for self-powered autonomous wireless sensors

Usman Khan, Ronan Hinchet, Hanjun Ryu, and Sang-Woo Kim[a]
School of Advanced Materials Science and Engineering, Sungkyunkwan University (SKKU), Suwon 440-746, South Korea

(Received 31 January 2017; accepted 28 March 2017; published online 14 April 2017)

Largely distributed networks of sensors based on the small electronics have great potential for health care, safety, and environmental monitoring. However, in order to have a maintenance free and sustainable operation, such wireless sensors have to be self-powered. Among various energies present in our environment, mechanical energy is widespread and can be harvested for powering the sensors. Piezoelectric and triboelectric nanogenerators (NGs) have been recently introduced for mechanical energy harvesting. Here we introduce the architecture and operational modes of self-powered autonomous wireless sensors. Thereafter, we review the piezoelectric and triboelectric NGs focusing on their working mechanism, structures, strategies, and materials. [http://dx.doi.org/10.1063/1.4979954]

I. INTRODUCTION

Electronic miniaturization inherently possesses the advantages of low cost, high speed, high density, light weight, and low power consumption. It, therefore, has revolutionized the development from large size vacuum tube computers to the today's personal and portable electronic devices such as cell phones, laptops, and tablets. The trend of miniaturization shall keep going to produce small electronics with extremely small size and ultra-low power consumption.[1,2] Micro-electro-mechanical systems (MEMS) and nano-electro-mechanical systems (NEMS) technologies are going to add additional functionalities, such as chemical, biological, tactile, acoustic, radiation, navigation, and flow sensing, to the small electronics. By taking advantage of communication technologies, the multifunctional small electronics can realize wireless sensor networks (WSNs) with great benefits in fields of health care, environmental and structural monitoring, security, nanorobotics, etc.[3,4]

Powering the huge number of the distributed sensor nodes in WSNs poses a great challenge. Batteries, however, do not offer a practical solution. They have a limited lifetime, so the huge numbers of replacements would be unrealistic. Additionally, since the battery materials are potentially hazardous, tracking and recycling of the huge number of batteries would be another big challenge.[1,3] Therefore, for an independent, maintenance-free operation, a power generator such as a nanogenerator (NG) has to be integrated within each sensor node in order to power them by harvesting energy from its working environment.[4,5]

The environment has an abundance of energies in the form of thermal, mechanical, solar, chemical energies, etc.[4] However, mechanical energy is available almost everywhere and anytime[6] especially in domestic, industrial, and transport environments where the sensor networks have numerous applications. Therefore, here, we focus on mechanical energy harvesting. In order to harvest mechanical energies in our environment, piezoelectric and triboelectric NGs have been introduced.[7,8] Significant progresses have been made for their development and have been the subject of various reviews as well.[1–4,6,9–13]

[a]Author to whom correspondence should be addressed. Electronic mail: kimsw1@skku.edu. Tel.: +82-31-290-7352. Fax: +82-31-290-7410.

II. SELF-POWERING AUTONOMOUS WIRELESS SENSOR

Sensors based on small electronics have a very low power consumption in the range of microwatts to milliwatts.[2,4] However, any information from the sensors has to be first processed and then transmitted to a central station in order to provide services such as environmental monitoring and health care.[2] Therefore, a controller/processor and a transmitter are indispensable for the operation of the sensors. However, these additional components require additional power as well. For instance, microcontrollers such as SAM L MCUs from Microchip Atmel consume power in microwatts.[14] On the other hand, the communication of any information can relatively have higher power consumptions.[2] For example, an RF transmitter such as CC1050 from Texas Instruments has a power consumption up to milliwatts and is capable of transmitting information at a rate of 76.8 kbaud.[15] Though NGs with peak power in milliwatts have been demonstrated,[16] the output is comprised of short duration pulses[8,17–19] and so the average power can be very low. As a consequence, NGs can have limitations for continuously powering a wireless sensor. Therefore, a self-powered wireless sensor also requires an energy storage device such as a battery or a capacitor in order to first store the energy from the NG and then periodically utilize it for its functioning. Figure 1(a) schematically describes a self-powered autonomous wireless sensor using an NG.

Practically, information from wireless sensors is only periodically required. For instance, a sampling rate of once every few hours is sufficient in order to monitor the water quality of a region. As a consequence, a wireless sensor can operate in active and sleep modes where the active mode is much shorter in duration and has much higher power consumption than its sleep mode.[2,4] Such low duty cycle operation of wireless sensors can be exploited to have a self-powered operation using NGs. The energy harvested from the NG can be stored during the sleep mode and later it can be utilized to power the wireless sensor during the active mode in order to perform sensing, data processing, and transmission. Figure 1(b) schematically describes the modes of operation of a self-powered autonomous wireless sensor.

III. PIEZOELECTRIC NGs

Piezoelectric NGs (PENGs) were first introduced in 2006 by Wang for mechanical energy harvesting.[7] When piezoelectric ZnO nanowires (NWs) were strained using a conductive atomic force microscope (AFM) tip, a potential was created across the NWs due to the separation of the static ionic charge centers.[7] The piezoelectric potential can be a driving force for a flow of current in an external circuit. Electrical contacts to the semiconducting ZnO NWs had a crucial importance. In fact, the AFM tip was required to have a Schottky contact with the NWs in order to prevent the current from entering the contact.[7]

PENGs based on ZnO NWs have the potential to harvest tiny forces over a broad frequency range from few Hz to several MHz and, therefore, are ideal for harvesting various mechanical energies coming from vibrations, human activity, gentile air flows, etc.[2,12,20,21] They are also environmental friendly as ZnO is non-toxic and biocompatible.[12] Several important progresses have been made for energy harvesting using PENGs since their introduction in 2006.[22–30] Initially, ZnO NWs based

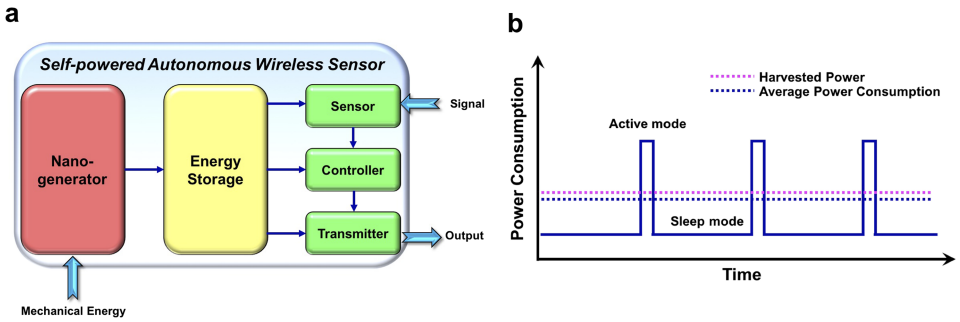

FIG. 1. (a) Schematic description and (b) operational modes of a self-powered autonomous wireless sensor. (b) is inspired from Ref. 2.

PENGs utilized a Schottky contact structure,[24] whereas, later, a sandwich structure[30] was introduced with significant advantages. Here, we shall outline both approaches in detail.

A. Schottky contact structure based PENGs

A PENG based on semiconducting ZnO NWs has a metal-semiconductor interface at each end of the NWs.[6,7] One of the interfaces has to be of Schottky type in order to prevent electrons to enter the interface.[7,24] Indeed, passing of electrons through the metal-semiconductor interface would potentially short circuit the two contacts. Therefore, in order to ensure a Schottky contact at one side, selection of a metal for the contact is to be based on its work function relative to the electron affinity of the semiconducting material.[6,20] As to the working mechanism, when stress is applied to the NG, a piezoelectric potential gradient is generated along the NWs and, as a consequence, the electrons flow in the external circuit and accumulate at the Schottky barrier of the NG. As the stress is removed, the piezoelectric potential disappears, and therefore the accumulated electrons flow in the opposite direction thereby generating an alternating current output.[6]

Here, we shall present vertical and lateral designs of the Schottky contract structure based PENGs.

1. Vertical nanowires array integrated NG

In 2010, Xu *et al.* demonstrated a vertical nanowire array integrated NG (VING).[24] The NG is comprised of vertical ZnO NWs with a platinum based Schottky contact at the top. Figure 2 presents the fabrication process and working of the NG. Vertically aligned ZnO NWs were grown on a gold-coated Si substrate using a low temperature hydrothermal growth method (see Figure 2(b)). Thereafter, a polymethylmethacrylate (PMMA) film was spin-coated onto the nanowires (see Figure 2(c)). The purpose of the PMMA film was partly to prevent the possible short-circuiting between the

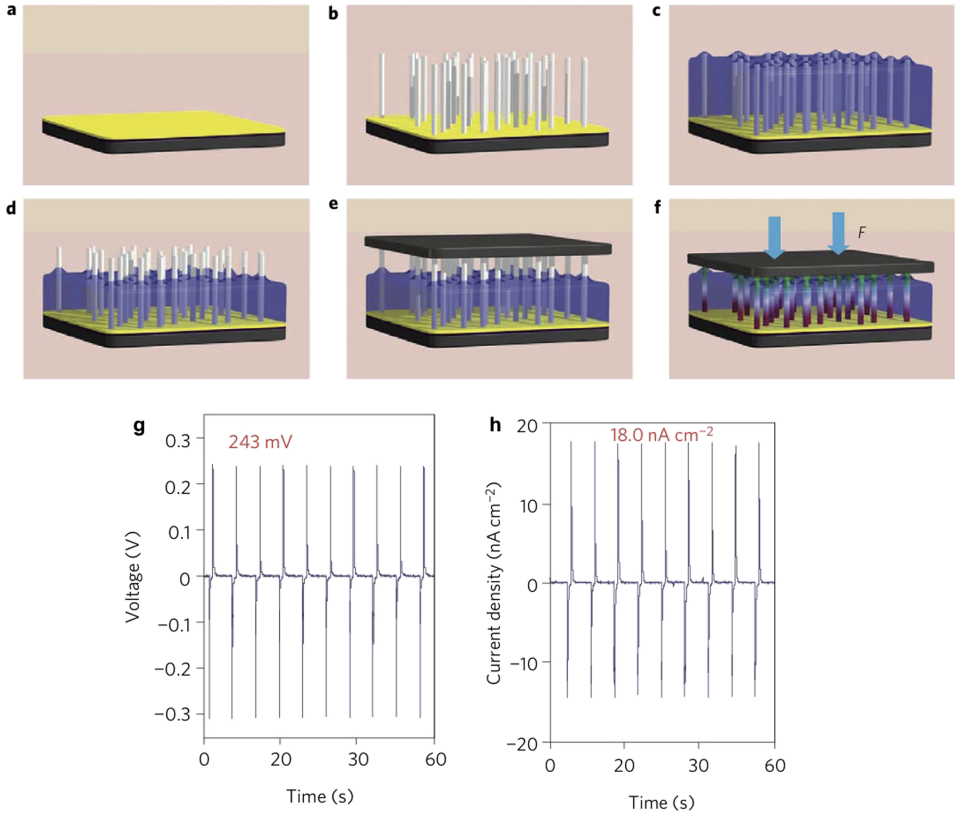

FIG. 2. Fabrication, working, and electrical output of the VING. (a) Au-coated silicon substrate. (b) ZnO NWs growth. (c) Spin coating of PMMA. (d) Exposing the NWs tips using oxygen plasma etching. (e) A Pt electrode to the NWs. (f) Piezoelectric potential along the NWs due to a compressive strain. (g) Output voltage from three VINGs connected in series. (h) Output current from three VINGs connected in parallel. Adapted with permission from Xu *et al.*, Nat. Nanotechnol. **5**, 366 (2010). Copyright 2010 Nature Publishing Group.

top and bottom electrodes and also to add mechanical robustness to the structure. Oxygen plasma etching was then carried out in order to expose the tips of the nanowires (see Figure 2(d)). Finally, in order to realize a Schottky contact at the top electrode, a platinum film (coated on a silicon wafer) was direct contacted with the nanowires (see Figure 2(e)).

When stress is applied on the VING, the NWs undergo a uniaxial compression and so a piezoelectric potential gradient is generated along their *c* axis (see Figure 2(f)). The device characterization has shown that three VINGs in a serial connection produce an output voltage of 0.243 V (see Figure 2(g)). Likewise, three VINGs in a parallel configuration generate an output current density of 18.0 nA cm^{-2} (see Figure 2(h)).

2. Lateral nanowires array integrated NG

Xu *et al.* demonstrated the lateral nanowire array integrated nanogenerator (LING).[24] LING is composed of lateral ZnO NWs with gold based a Schottky contact at one end. Figure 3 presents the fabrication process, the working mechanism, and the electrical output of the NG. Laterally aligned ZnO NWs were grown parallel to the substrate on a ZnO seed layer using a low temperature chemical growth method (see Figure 3(a)). On one side of the nanowires, a thick layer of gold was deposited in order to realize the Schottky electrode (see Figure 3(b)). The device design of the LING (shown in Figure 3(b)) is meant to enhance the output power by integrating the outputs from multiple NWs. When the substrate is stretched, nanowires undergo a tensile strain and therefore produce a piezoelectric potential as shown in Figure 3(c). In order to characterize the LING, a periodic external force was applied to the flexible substrate such that the NWs undergo a cyclic stretching–releasing. Figures 3(d) and 3(e) show the corresponding output voltage and current, respectively, of an LING composed of 700 rows of NWs; the LING produced an average output voltage of 1.2 V and a current pulse of 26 nA.

3. Issues of the Schottky contact structure based PENGs

PENGs based on the Schottky contact design have several limitations.[6,20,30] First, such devices may suffer from strong mechanical aging as a metal-nanowire contact is inherently hard and so can greatly deteriorate with repeated usage.[6,20] Another major concern is stability and reproducibility of such PENGs due to typical attributes of Schottky interfaces.[6] In fact, apart from the work function difference of the two materials, Schottky contacts are also influenced by the metal-semiconductor interface states.[6] Moreover, such contacts are also affected by the environmental parameters.[6] Additionally, they also add complexity to the fabrication process.[6]

B. Sandwich structure based PENGs

Sandwich structure design comprises a composite of piezoelectric NWs and a polymer, such as PMMA, sandwiched between two electrodes.[30,31] As a consequence, the Schottky contact is replaced

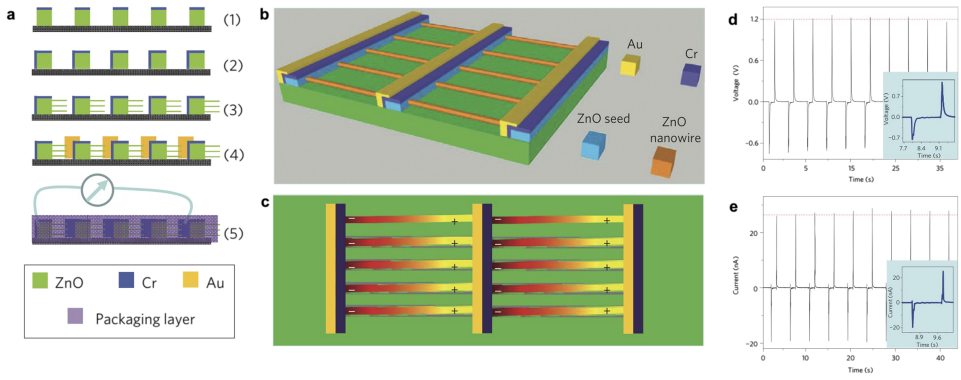

FIG. 3. Fabrication process, device design, working mechanism, and electrical output of the LING. (a) Schematic description of ZnO NWs growth and the deposition of Au electrodes. (b) LING device schematic. (c) Piezoelectric potential under mechanical deformation. Output voltage (d) and output current (e) of the LING comprising 700 rows of NW arrays. Adapted with permission from Xu *et al.*, Nat. Nanotechnol. **5**, 366 (2010). Copyright 2010 Nature Publishing Group.

by a thin insulating layer that offers an infinitely high potential barrier and therefore effectively prevents electrons to enter the interface with ZnO NWs.[6,30] As to the working mechanism, when the NG is subjected to a stress, a piezoelectric potential field is created along the NWs. Due to electrostatic induction, charges flow across the external circuit and accumulate on the top and bottom electrodes in order to screen the piezoelectric potential.[20,27] When the stress is released, the piezoelectric potential diminishes and therefore the accumulated charges flow back through the external circuit.[20,27] The sandwich structure design offers crucial advantages. First, the polymer can potentially enhance the transmission of the mechanical energies to all of the NWs and therefore offer the possibility of realizing high efficiency and high output PENGs.[6,20,32] Furthermore, the incorporation of polymers adds mechanical robustness to the devices as it prevents NWs from direct contact with the electrode.[6,20]

Zhu *et al.* demonstrated a sandwich structure based PENG[30] for harvesting mechanical energies from vertical compression.[30] Figure 4 shows the fabrication process, the device prototype, and the electrical output. A silicon wafer was first deposited with an ITO electrode and then with a ZnO seed layer (see Figures 4(a)–4(c)). Thereafter, a layer of photoresist was patterned using photolithography (see Figure 4(d)) and ZnO NWs were grown on the exposed seed surface using the wet chemical method (see Figure 4(e)). Residual photoresist was then removed, and NWs were thermally annealed (see Figure 4(f)). A layer of PMMA was spin-coated on the NWs, and an aluminum film was deposited as a top electrode (see Figures 4(g) and 4(h)). Finally, the NG was packaged in another layer of PMMA (see Figure 4(i)). Figure 4(j) shows an energy harvesting pad that consists of nine NGs connected in parallel. The PENG produces a peak output voltage and a current of 58 V and 134 μA, respectively, when punched by a human palm (see Figures 4(k) and 4(i)). It is evident that the electrical power of

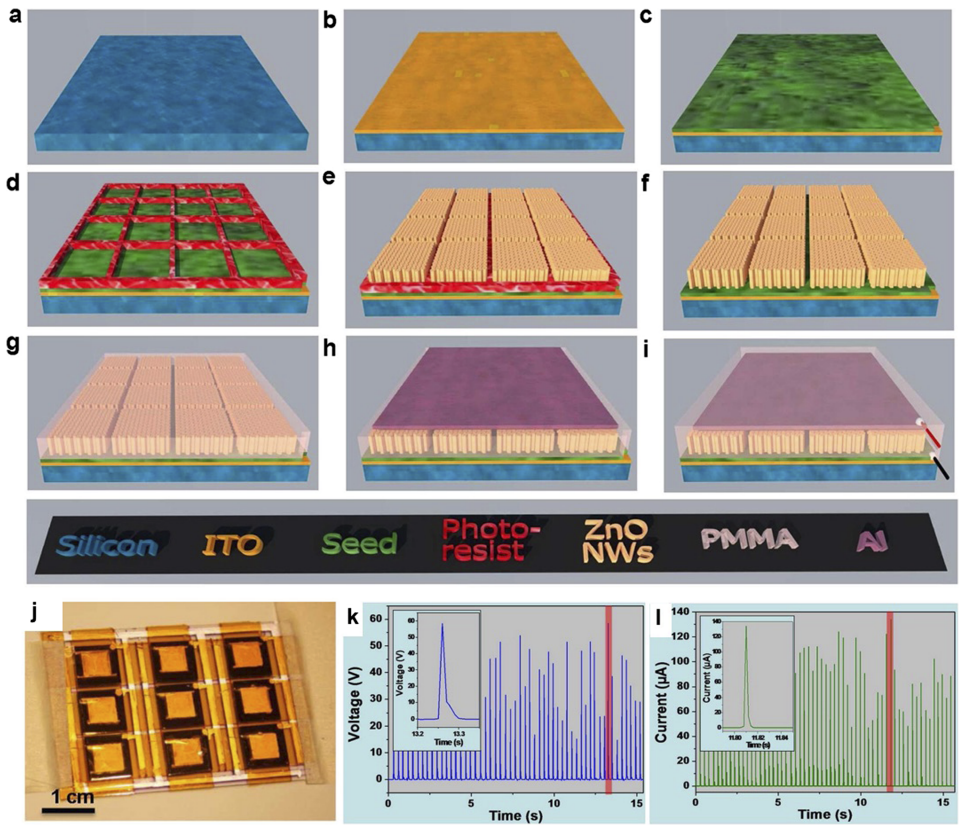

FIG. 4. Fabrication process, prototype, and electrical output of a sandwich structure based PENG. (a) Silicon substrate. Deposition of (b) ITO electrode, and (c) ZnO seed layer. (d) Patterning photoresist for creating windows. (e) ZnO NWs' growth. (f) Removal of residual photoresist. (g) Spin-coating PMMA layer. (h) Al electrode deposition. (i) Device packaging by spin-coating PMMA. (j) A pad with nine NGs in parallel. Rectified output voltage (k) and (l) current of the NG pad due to impact by a human palm. Adapted with permission from Zhu *et al.*, Nano Lett. **12**, 3086 (2012). Copyright (2012) American Chemical Society.

the sandwich structure design is significantly higher in comparison to that of the Schottky contact design.[22–25]

C. Materials for PENGs

Since the initial studies on piezoelectric properties of ZnO NWs in 2006,[7] several materials have been investigated for mechanical energy harvesting using PENGs. Significant research efforts have focused on piezoelectric semiconducting materials such as ZnO,[7,24,27] CdS,[33,34] and GaN.[35–37] However, ZnO can be grown using hydrothermal synthesis which is simple, low cost, and low temperature (under 100 °C).[38] Low temperature nature of the process is extremely useful, for instance, for integration on flexible substrates for flexible PENGs. Materials with a perovskite structure such as lead zirconate titanate (PZT),[39,40] and barium titanate,[41,42] which possess high piezo-electric coefficient (d_{33}) value,[12] have also been studied for PENGs. However, in comparison to PZT, barium titanate is eco-friendly as it is lead free. PENGs based on polymer-based piezoelectric materials, such as polyvinylidene fluoride (PVDF) and its copolymer poly[vinylidenefluoride-co-trifluoroethylene], have also been demonstrated.[12,43,44] Such devices have the unique advantages of flexibility and biocompatibility which are highly desired for implantable energy harvesting applications.[12,43] However, they require electrical poling in order to align the dipoles of the polar β-phase of PVDF structures. Recently, 2D transition metal dichalcogenides (TMDs) such as MoS_2 have also been investigated for mechanical energy harvesting using a piezoelectric phenomenon.[45–47] Layer control is crucial for such NGs; in fact, the piezoelectric output is highest with monolayer and decreases with the number of odd layers; whereas no output is generated with even number of layers.[45]

IV. TRIBOELECTRIC NGs

When two distinct materials come into contact with each other, their surfaces are electrically charged with opposite polarities in a process known as triboelectrification.[48–50] Polarity of the triboelectric charges on the surface of the contacting materials is determined by their relative tendency to lose/gain electrons.[3,51,52] Insulators are generally known to undergo strong triboelectrification, and they retain the triboelectric charges over long periods.[1] In 2012, Chi Zhang *et al.* introduced triboelectric NGs (TENGs) that utilize the triboelectric charges as a driving force for a current flow in an external circuit through electrostatic induction.[8] Such coupling of triboelectrification and electrostatic induction has found great prospects for TENGs in the field of mechanical energy harvesting.

The choices for the pair of friction materials in a TENG are huge as every material exhibits triboelectricity.[1,51] However, the two materials should be largely separated in the triboelectric series in order to have high output in TENGs.[8,53] TENGs are simple, easy to fabricate, low cost, and mechanically robust.[8,9,54,55] TENGs with efficiency as high as 85%[56] and power as high as 500 W/m^2 [57] have also been demonstrated. TENGs have four working modes of vertical contact separation, contact sliding, single electrode, and the freestanding triboelectric-layer mode (see Figure 5).[3,9] TENGs, therefore, can be adapted to harvest various types of mechanical energies such as touching,[58,59] sliding,[57,60] rotation,[61,62] impact,[63,64] and vibration[16,65] coming from human motion, wind, ocean waves and tides, sound, moving automobiles, flowing water, etc.[9,66,67] Due to the unique advantages, TENGs have great potential for self-powering sensors.

Here, we shall discuss in detail the four working modes of TENGs and various strategies for high output performance.

A. Four operational modes of TENGs

1. Vertical contact separation mode TENGs

The vertical contact separation mode of TENG is schematically described in Figure 5(a). Such TENGs consist of a pair of dielectric layers facing each other in a vertical fashion.[3,68,69] Electrodes are deposited on their back/other sides and are interconnected to form an external circuit. A metal-dielectric pair[70] is also utilized as the friction layers in TENGs as metals have more free electrons to transfer during triboelectrification. When an external force brings the two friction layers into contact, they are oppositely charged due to triboelectrification. At the moment of contact, the opposite charges on their surfaces neutralize each other and therefore there is no net field. When the two layers separate

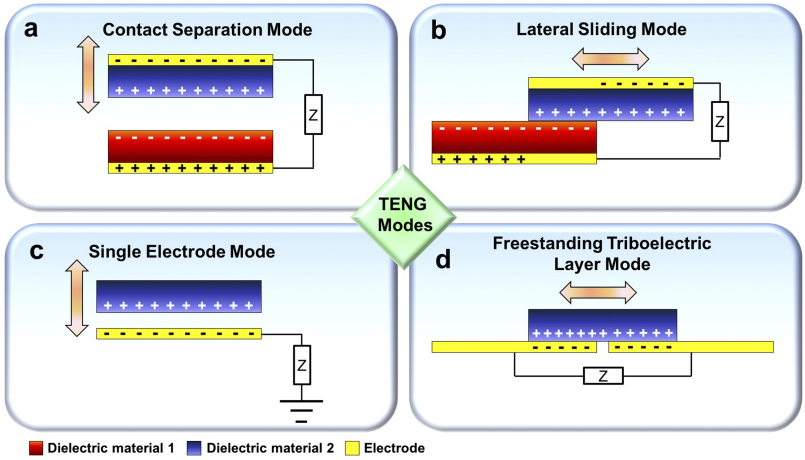

FIG. 5. Four operational modes of TENGs. (a) Vertical contact separation mode. (b) Contact sliding mode. (c) Single electrode mode. (d) Freestanding triboelectric layer mode (inspired from Refs. 3 and 9).

due to removal of the external force, the triboelectric charges electrostatically induce opposite charges on the electrodes and, as a consequence, current flows in the external circuit. When the layers come into contact again, the opposite charges once again neutralize each other and so the electrostatic field disappears and the current flows in the opposite direction thereby producing an alternating current.

As a representative of contact separation mode TENGs, here we present the transparent and flexible graphene triboelectric NG (GTNG) demonstrated by Kim *et al.* in 2014.[71] GTNG consists of graphene and polyethylene terephthalate (PET) as the triboelectric layers; another graphene layer serves as the back electrode of the PET layer (see Figure 6). Graphene was first grown on a metallic foil (copper or nickel) using chemical vapor deposition (CVD) (see Figure 6(a)). Thereafter, the graphene was transferred onto a PET substrate using the standard wet transfer method (see Figure 6(b)). Finally, in order to realize the complete device, two of such substrates were stacked in a vertical way with 0.8 mm plastic spacers in between (see Figures 6(c)–7(d)). The electrical characterization of the GTNG is shown in Figures 6(e) and 7(f). When subjected to a force of 1 kgf, GTNG produces a peak output voltage and a current density of 5 V and 0.5 μA cm^{-2}, respectively, with a single layer (1L) CVD graphene grown on the Cu foil. However, the outputs decrease with an increase in the number of the graphene layers (see Figures 6(e) and 7(f)); the multilayer graphene was realized by stacking several single layer graphene layers.

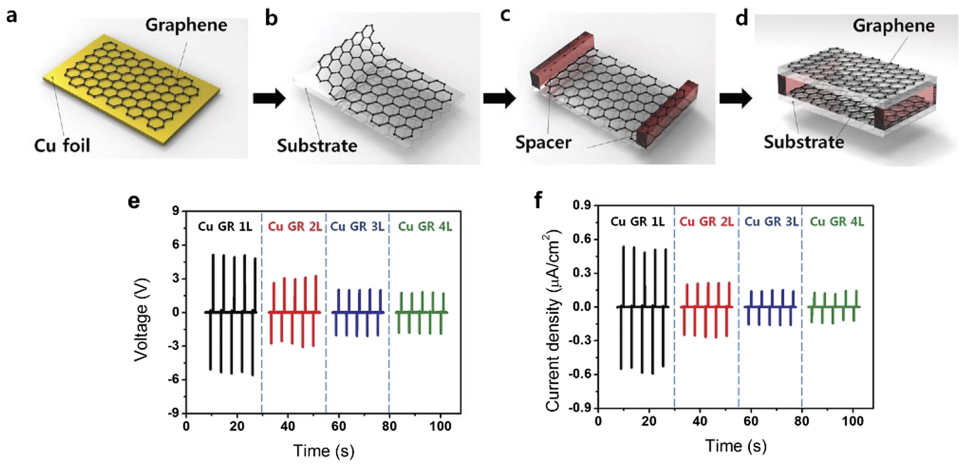

FIG. 6. Device fabrication and electrical output of GTNG. (a) CVD-graphene grown on the Cu-foil. (b) Graphene transfer onto the PET substrate. (c) Plastic spacers for gap. (d) Placing another PET/graphene to complete the device. (e) Output voltage and (f) current density of the NG under a vertical compressive force of 1 kgf; 1L, 2L, 3L, and 4L denote one, two, three and four layers of graphene. Adapted with permission from Kim *et al.*, Adv. Mater. **26**, 3918 (2014). Copyright 2014 Wiley.

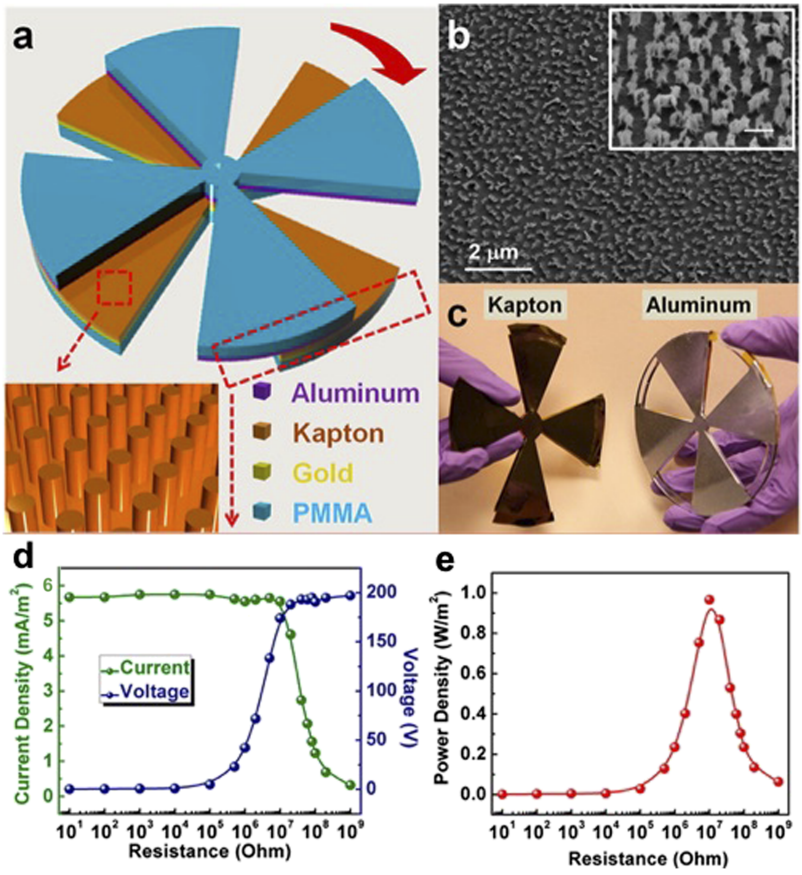

FIG. 7. Device structure and electrical output of a contact sliding mode TENG. (a) Device schematic; inset shows the Kapton nanorods created on the surface. (b) SEM image of the Kapton nanorods; the inset is a high magnification SEM image; the scale bar is 500 nm. (c) The two parts of the fabricated TENG. (d) Output voltage and current density as a function of load resistance. (e) Output power density as a function of load resistance. Adapted with permission from Lin *et al.*, Nano Lett. **13**, 2916 (2013). Copyright (2013) American Chemical Society.

2. Contact sliding mode TENGs

Contact sliding mode TENG is schematically described in Figure 5(b) where the two friction layers slide upon each other due to external forces.[60] As the friction layers start sliding apart, the unscreened triboelectric charges on their inner surfaces start electrostatically inducing opposite charges on the electrodes thereby causing a current flow in the external circuit. A periodic sliding in and out of the friction layers generates an alternating current in the external circuit. The contact sliding mode can be adapted to have the relative sliding in a planar, rotational, and cylindrical fashion.[72] Linear grating[72] and circular segmentation[61] of the triboelectric layers can greatly enhance the output performance of contact sliding mode TENGs. Indeed, grated and segmented triboelectric layers only require a sliding of a length of a grating or a segment to fully mismatch. Therefore, when the two layers fully separate, the charge transfer occurs multiple times and accordingly the current transport efficiency is also increased.

As a representative design of contact sliding mode TENGs, we present a segmented disc shaped TENG reported by Long Lin *et al.* in 2013 for harvesting rotational mechanical energy.[61] The TENG design consists of two discs with four segments each as shown in Figure 7(a). A Kapton film and an aluminum (Al) sheet comprise a triboelectric pair of the TENG, whereas a gold (Au) film acts as the back electrode of the Kapton film. In order to enhance the contact area and therefore the output power, an array of nanorods were realized on the Kapton film using inductive coupled plasma (ICP) reactive ion etching as shown in Figure 7(b); the Kapton nanorods have an average diameter and length of 150 and 600 nm, respectively. The segmented disk type TENG design undergoes multiple

charge transfers within a full rotation cycle. Figure 7(d) shows the output current density and output voltage of the TENG as a function of the load resistance. Figure 7(e) shows the output power density of the device as a function of the load resistance. The TENG has a maximum power density of ~1 W/m^2.

3. Single electrode mode TENGs

The electrodes in contact sliding and contact separation mode TENGs are interconnected and therefore they may have design limitations in some cases. For instance, in order to harvest mechanical energies from human walking on a floor, moving automobiles, finger typing or finger sliding over touch screens, etc, one of the friction layers is freely moving and therefore the electrodes cannot be interconnected. In order to overcome the challenge, the single electrode mode TENG has been introduced.[58,59,73,74] Such a design has a single friction layer with a back electrode connected to ground as schematically described in Figure 5(c). The external object, that either contacts or slides on the TENG, acts as the complementary friction layer. Periodic mechanical energies in the form of contact-separation or relative sliding result into an alternating current between the electrode and the ground.

Meng *et al.* demonstrated a single electrode mode TENG.[75] The TENG comprises a single micro-structured Polydimethylsiloxane (PDMS) or flat PET film as the friction surface. The external freely moving object serves as the second friction surface in the friction pair. Figure 8(a) shows a schematic diagram of the TENG. The PDMS film is patterned with an array of micro-pyramids (see the SEM image in Figure 8(b)) and is fabricated on a 125 μm thick PET substrate. Besides, the TENG has an ITO based electrode coated on the back side of the PET substrate. A 100 μm thick grounded copper foil acts as a reference electrode. Figure 8(c) shows a fabricated TENG demonstrating its flexibility and transparency.

Figure 8(d) describes the working mechanism of the TENG. Upon contact, the friction pair is electrically charged with opposite polarities. When the external object separates from the friction surface, a potential difference is created between the ITO electrode and the grounded reference

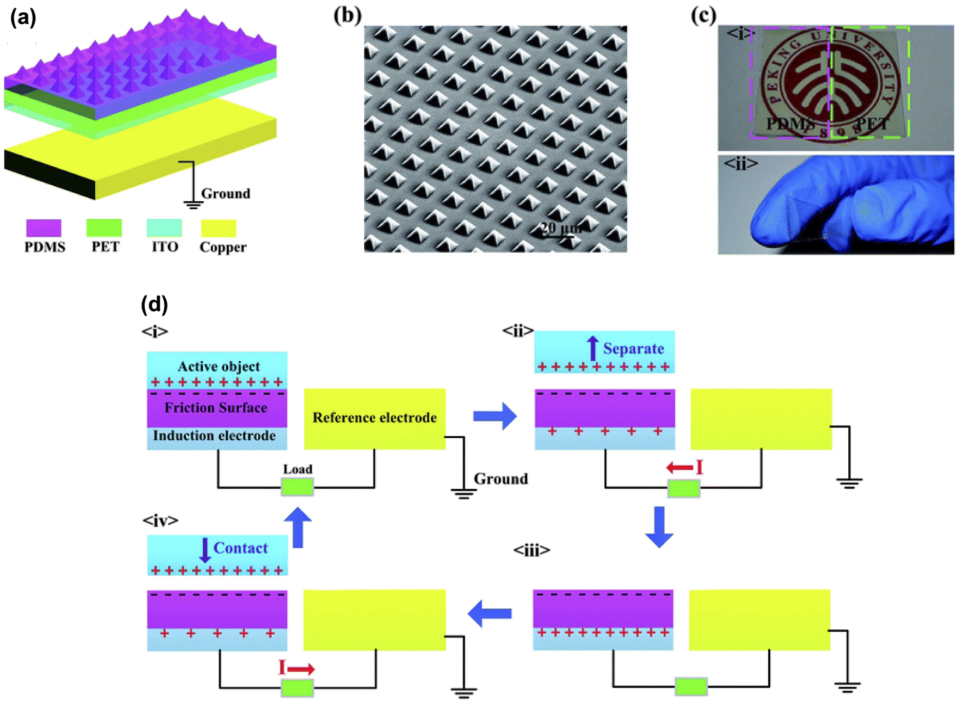

FIG. 8. Device structure, working mechanism of the single electrode mode TENG. (a) Schematic of the device. (b) SEM image of the micro-structured PDMS friction layer. (c) TENG's photographs showing transparency and flexibility. (d) Working mechanism of the TENG. Reproduced with permission from Meng *et al.*, Energy Environ. Sci. **6**, 3235 (2013). Copyright 2013 Royal Society of Chemistry.

electrode. As a consequence, current flows from one electrode to the other. As the active object contacts the friction surface again, the current flows in the opposite direction. Figure 8(d) shows the case when the friction layer of the device has higher tendency than the external object to attract electrons and therefore is negatively charged. When the TENG was tapped with a bare finger, it produced a peak open circuit voltage and a peak short circuit current of ~140 V and ~5 μA, respectively, which demonstrates the suitability of the TENG design for harvesting mechanical energy from freely moving objects.

4. Free-standing triboelectric layer mode TENGs

Free-standing triboelectric layer mode TENG is schematically described in Figure 5(d). Like the single electrode mode, such a TENG design is well suited to harvest mechanical energies from freely moving objects. Indeed, freely moving objects comprise the free-standing triboelectric layer of the TENGs.[76] Additionally, the TENG design consists of an interconnected pair of electrodes whose size should be such that the free-standing layer can only cover either of them.[56,62,76] When the free-standing layer comes into contact with either of the electrodes, the current flows between them due to the varying electrostatic field. The free-standing layer can slide on the electrodes in both the planar[76] and rotational manner.[62] Instead of the laterally aligned configuration (as in Figure 5(d)), the electrodes can also be oriented in vertical configuration with a free-standing layer moving in between them.[77] In case the free-standing layer is electrically conductive, the TENG then requires a dielectric layer with the electrode underneath.[77] Free-standing layer mode TENGs can also operate in the non-contact mode.[76] Indeed, once the triboelectric layers are charged by an initial contact[9] then the contact sliding is not necessary anymore. For instance, the free-standing layer can also slide over the electrodes, however, keeping an adequate separation.[76] Such a non-contact operation of the TENGs can greatly extend the lifetime by reducing the surface wearing due to sliding motion.[76]

As a representative design of the freestanding layer mode, we present the TENG demonstrated by Kim *et al.* in 2015.[78] The TENG consists of polytetrafluoroethylene (PTFE) powder as a freestanding triboelectric material (see Figure 9(a)). Two Al metal plates act as the top and bottom electrodes of the TENG. An acrylic cylinder is placed between the two metal electrodes. The TENG is composed of two additional pairs of copper tape electrodes that are attached onto the outer side wall of the acrylic cylinder. In order to enhance the triboelectric output, vertical nanowires were realized on the Al electrode as shown in Figure 9(b). Though the TENG can harvest energy from mechanical vibrations in the x-, y-, and z-directions, here, we focus on the vertical vibrations, i.e., along the z-direction, of the free-standing layer; besides, the TENG's output can potentially be higher due to vertical vibrations as the contact area is relatively higher than in the other directions. Figure 9(e) describes the working mechanism in the case of vertical vibration of the free-standing layer. Upon contact with an Al plate, the free-standing layer is negatively charged, whereas the Al plate is positively charged. Under the influence of a vertical force, the free-standing powder periodically contacts and separates from the top and the bottom electrodes, and, as a consequence, an alternating current flows between the electrodes due to electrostatic induction. A vertical vibration at a frequency of 3 Hz produces an open-circuit voltage and a short-circuit current of 245 V and 10 μA, respectively, as shown in Figure 9(f).

B. Surface treatments for enhancing TENG's output

In order to have high output power from TENGs, the triboelectric materials should be from the opposite sides of the triboelectric series.[53] Besides, surface treatments are also utilized in order to further enhance the performance. Surface treatments are mainly of two kinds: surface functionalization and surface morphology control. Surface functionalization aims at modifying the surface potential of triboelectric materials in order to enhance the triboelectric output.[79] Indeed, the surface of a triboelectric material can be chemically functionalized with various functional groups such as $-NH_2$, $-SH$, $-CH_3$, and $-CF_3$[79,80] in order to enhance the electron donating or electron receiving ability during triboelectrification. Li *et al.* fluorinated the surface of PET in a TENG based on PET-copper as a triboelectric pair.[81] The surface treatment resulted in an enhancement of ~300% in the open-circuit voltage and short-circuit current of the TENG.

Surface morphology control is about modifying the surfaces of triboelectric layers by physical treatments in order to enhance the contact area.[3,53] Indeed, the increase in the contact area potentially increases the triboelectric charge density and therefore the output of TENGs. Generally, triboelectric

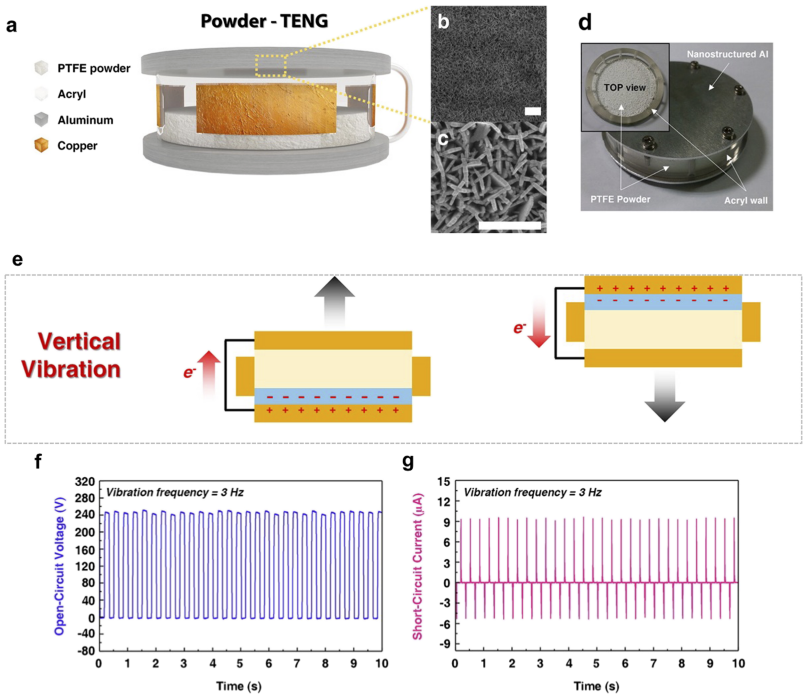

FIG. 9. Device structure, working mechanism, and output performance of the freestanding triboelectric layer TENG. (a) Device schematic. ((b) and (c)) SEM image showing nanostructures on Al; scale bars are 500 nm. (d) Fabricated TENG. (e) Working mechanism of the TENG under vertical vibration. (a) Open-circuit voltage and (b) short-circuit current of the TENG at a vibration frequency of 3 Hz. Adapted with permission from Kim *et al.*, ACS Nano **10**, 1017 (2016). Copyright (2016) American Chemical Society.

layers are patterned with micro- and nanostructures such as pyramids,[54] cubes,[54] semi-spheres,[82] and nanopatterns[18,83] in order to enhance the contact area of triboelectrification. Lee *et al.* recently demonstrated a TENG with polyurethane (PU) and aluminum as triboelectric materials.[84] The output voltage of the TENG with micro-pyramid pattering was 20 times higher than the one with a flat PU surface. This demonstrates that the surface morphology control can greatly enhance the output performance of TENGs.

V. SUMMARY

Networks of small electronics based sensors can greatly benefit our lives in the fields of health care, environmental and structural monitoring, safety and security, etc. However, the largely distributed sensors have to be self-powered using NGs as batteries have a limited lifetime and the number of required replacements could be gigantic. Among various energies present in our environment, mechanical energy is present almost everywhere and anytime, particularly in domestic, industrial, and transport environments where the sensors have crucial applications. PENGs and TENGs are two of the major technologies for mechanical energy harvesting. In this paper, we have discussed the architecture and working of a self-powered autonomous wireless sensor. Additionally, we reviewed PENGs and TENGs where we have thoroughly discussed their working mechanism, the design structures, strategies for enhancing the output performance, and candidate materials.

ACKNOWLEDGMENTS

This work was financially supported by the Industrial Strategic Technology Development Program (No. 10052668, Development of wearable self-powered energy source and low-power wireless communication system for a pacemaker) and "Human Resources Program in Energy Technology" of the Korea Institute of Energy Technology Evaluation and Planning (KETEP, No. 20154030200870),

and was granted financial resource from the Ministry of Trade, Industry & Energy (MI, Korea). R.H. acknowledges support from Research Fellow Program (No. 2015R1D1A4A01020840) through the National Research Foundation (NRF) of Korea Grant funded by the Ministry of Science, ICT & Future Planning.

[1] Z. L. Wang, ACS Nano **7**, 9533 (2013).
[2] Z. L. Wang and W. Wu, Angew. Chem., Int. Ed. **51**, 11700 (2012).
[3] R. Hinchet, W. Seung, and S. Kim, ChemSusChem **8**, 2327 (2015).
[4] Z. L. Wang, Adv. Mater. **24**, 280 (2012).
[5] J.-H. Lee, J. Kim, T. Y. Kim, M. S. Al Hossain, S.-W. Kim, and J. H. Kim, J. Mater. Chem. A **4**, 7983 (2016).
[6] Y. Hu and Z. L. Wang, Nano Energy **14**, 3 (2015).
[7] Z. L. Wang, Science **312**, 242 (2006).
[8] F.-R. Fan, Z.-Q. Tian, and Z. Lin Wang, Nano Energy **1**, 328 (2012).
[9] Z. L. Wang, Faraday Discuss. **176**, 447 (2014).
[10] X.-S. Zhang, M.-D. Han, B. Meng, and H.-X. Zhang, Nano Energy **11**, 304 (2015).
[11] Z. L. Wang, J. Chen, and L. Lin, Energy Environ. Sci. **8**, 2250 (2015).
[12] K. Y. Lee, M. K. Gupta, and S.-W. Kim, Nano Energy **14**, 139 (2015).
[13] F. R. Fan, W. Tang, and Z. L. Wang, Adv. Mater. **28**, 4283 (2016).
[14] See http://www.atmel.com/products/microcontrollers/ARM/SAM-L.aspx for Microchip Atmel.
[15] See http://www.ti.com/product/CC1050 for Texas Instruments.
[16] J. Chen, G. Zhu, W. Yang, Q. Jing, P. Bai, Y. Yang, T.-C. Hou, and Z. L. Wang, Adv. Mater. **25**, 6094 (2013).
[17] F. Yi, L. Lin, S. Niu, P. K. Yang, Z. Wang, J. Chen, Y. Zhou, Y. Zi, J. Wang, Q. Liao, Y. Zhang, and Z. L. Wang, Adv. Funct. Mater. **25**, 3688 (2015).
[18] P. Bai, G. Zhu, Q. Jing, J. Yang, J. Chen, Y. Su, J. Ma, G. Zhang, and Z. L. Wang, Adv. Funct. Mater. **24**, 5807 (2014).
[19] A. Ahmed, Z. Saadatnia, I. Hassan, Y. Zi, Y. Xi, X. He, J. Zu, and Z. L. Wang, Adv. Energy Mater. 1601705 (2016).
[20] Z. L. Wang, G. Zhu, Y. Yang, S. Wang, and C. Pan, Mater. Today **15**, 532 (2012).
[21] B. Y. Lee, J. Zhang, C. Zueger, W.-J. Chung, S. Y. Yoo, E. Wang, J. Meyer, R. Ramesh, and S.-W. Lee, Nat. Nanotechnol. **7**, 351 (2012).
[22] X. Wang, J. Song, J. Liu, and Z. L. Wang, Science **316**, 102 (2007).
[23] S. Xu, Y. Wei, J. Liu, R. Yang, and Z. L. Wang, Nano Lett. **8**, 4027 (2008).
[24] S. Xu, Y. Qin, C. Xu, Y. Wei, R. Yang, and Z. L. Wang, Nat. Nanotechnol. **5**, 366 (2010).
[25] G. Zhu, R. Yang, S. Wang, and Z. L. Wang, Nano Lett. **10**, 3151 (2010).
[26] Y. Hu, Y. Zhang, C. Xu, G. Zhu, and Z. L. Wang, Nano Lett. **10**, 5025 (2010).
[27] Y. Hu, Y. Zhang, C. Xu, L. Lin, R. L. Snyder, and Z. L. Wang, Nano Lett. **11**, 2572 (2011).
[28] Y. Qin, X. Wang, and Z. L. Wang, Nature **451**, 809 (2008).
[29] D. Choi, M.-Y. Choi, W. M. Choi, H.-J. Shin, H.-K. Park, J.-S. Seo, J. Park, S.-M. Yoon, S. J. Chae, Y. H. Lee, S.-W. Kim, J.-Y. Choi, S. Y. Lee, and J. M. Kim, Adv. Mater. **22**, 2187 (2010).
[30] G. Zhu, A. C. Wang, Y. Liu, Y. Zhou, and Z. L. Wang, Nano Lett. **12**, 3086 (2012).
[31] K. Y. Lee, D. Kim, J.-H. Lee, T. Y. Kim, M. K. Gupta, and S.-W. Kim, Adv. Funct. Mater. **24**, 37 (2014).
[32] R. Hinchet, S. Lee, G. Ardila, L. Montès, M. Mouis, and Z. L. Wang, Adv. Funct. Mater. **24**, 971 (2014).
[33] Y.-F. Lin, J. Song, Y. Ding, S.-Y. Lu, and Z. L. Wang, Appl. Phys. Lett. **92**, 022105 (2008).
[34] Y.-F. Lin, J. Song, Y. Ding, S.-Y. Lu, and Z. L. Wang, Adv. Mater. **20**, 3127 (2008).
[35] C.-Y. Chen, G. Zhu, Y. Hu, J.-W. Yu, J. Song, K.-Y. Cheng, L.-H. Peng, L.-J. Chou, and Z. L. Wang, ACS Nano **6**, 5687 (2012).
[36] C.-T. Huang, J. Song, W.-F. Lee, Y. Ding, Z. Gao, Y. Hao, L.-J. Chen, and Z. L. Wang, J. Am. Chem. Soc. **132**, 4766 (2010).
[37] L. Lin, C.-H. Lai, Y. Hu, Y. Zhang, X. Wang, C. Xu, R. L. Snyder, L.-J. Chen, and Z. L. Wang, Nanotechnology **22**, 475401 (2011).
[38] S. Xu, N. Adiga, S. Ba, T. Dasgupta, C. F. J. Wu, and Z. L. Wang, ACS Nano **3**, 1803 (2009).
[39] Y. Qi, J. Kim, T. D. Nguyen, B. Lisko, P. K. Purohit, and M. C. McAlpine, Nano Lett. **11**, 1331 (2011).
[40] Y. Qi, N. T. Jafferis, K. Lyons, C. M. Lee, H. Ahmad, and M. C. McAlpine, Nano Lett. **10**, 524 (2010).
[41] Z.-H. Lin, Y. Yang, J. M. Wu, Y. Liu, F. Zhang, and Z. L. Wang, J. Phys. Chem. Lett. **3**, 3599 (2012).
[42] K.-I. Park, S. Xu, Y. Liu, G.-T. Hwang, S.-J. L. Kang, Z. L. Wang, and K. J. Lee, Nano Lett. **10**, 4939 (2010).
[43] C. Chang, V. H. Tran, J. Wang, Y.-K. Fuh, and L. Lin, Nano Lett. **10**, 726 (2010).
[44] J.-H. Lee, K. Y. Lee, M. K. Gupta, T. Y. Kim, D.-Y. Lee, J. Oh, C. Ryu, W. J. Yoo, C.-Y. Kang, S.-J. Yoon, J.-B. Yoo, and S.-W. Kim, Adv. Mater. **26**, 765 (2014).
[45] H. Zhu, Y. Wang, J. Xiao, M. Liu, S. Xiong, Z. J. Wong, Z. Ye, Y. Ye, X. Yin, and X. Zhang, Nat. Nanotechnol. **10**, 151 (2014).
[46] K.-A. N. Duerloo, M. T. Ong, and E. J. Reed, J. Phys. Chem. Lett. **3**, 2871 (2012).
[47] S. K. Kim, R. Bhatia, T.-H. Kim, D. Seol, J. H. Kim, H. Kim, W. Seung, Y. Kim, Y. H. Lee, and S.-W. Kim, Nano Energy **22**, 483 (2016).
[48] G. S. P. Castle, J. Electrost. **40–41**, 13 (1997).
[49] A. F. Diaz and R. M. Felix-Navarro, J. Electrost. **62**, 277 (2004).
[50] J. A. Wiles, B. A. Grzybowski, A. Winkleman, and G. M. Whitesides, Anal. Chem. **75**, 4859 (2003).
[51] D. K. Davies, J. Phys. D. Appl. Phys. **2**, 1533 (1969).
[52] J. Henniker, Nature **196**, 474 (1962).
[53] C. Zhang, W. Tang, C. Han, F. Fan, and Z. L. Wang, Adv. Mater. **26**, 3580 (2014).
[54] F.-R. Fan, L. Lin, G. Zhu, W. Wu, R. Zhang, and Z. L. Wang, Nano Lett. **12**, 3109 (2012).

[55] K. Y. Lee, J. Chun, J.-H. Lee, K. N. Kim, N.-R. Kang, J.-Y. Kim, M. H. Kim, K.-S. Shin, M. K. Gupta, J. M. Baik, and S.-W. Kim, Adv. Mater. **26**, 5037 (2014).
[56] Y. Xie, S. Wang, S. Niu, L. Lin, Q. Jing, J. Yang, Z. Wu, and Z. L. Wang, Adv. Mater. **26**, 6599 (2014).
[57] G. Zhu, Y. S. Zhou, P. Bai, X. S. Meng, Q. Jing, J. Chen, and Z. L. Wang, Adv. Mater. **26**, 3788 (2014).
[58] Y. Yang, H. Zhang, Z.-H. Lin, Y. S. Zhou, Q. Jing, Y. Su, J. Yang, J. Chen, C. Hu, and Z. L. Wang, ACS Nano **7**, 9213 (2013).
[59] G. Zhu, W. Q. Yang, T. Zhang, Q. Jing, J. Chen, Y. S. Zhou, P. Bai, and Z. L. Wang, Nano Lett. **14**, 3208 (2014).
[60] S. Wang, L. Lin, Y. Xie, Q. Jing, S. Niu, and Z. L. Wang, Nano Lett. **13**, 2226 (2013).
[61] L. Lin, S. Wang, Y. Xie, Q. Jing, S. Niu, Y. Hu, and Z. L. Wang, Nano Lett. **13**, 2916 (2013).
[62] L. Lin, S. Wang, S. Niu, C. Liu, Y. Xie, and Z. L. Wang, ACS Appl. Mater. Interfaces **6**, 3031 (2014).
[63] G. Zhu, Z.-H. Lin, Q. Jing, P. Bai, C. Pan, Y. Yang, Y. Zhou, and Z. L. Wang, Nano Lett. **13**, 847 (2013).
[64] L. Lin, Y. Xie, S. Wang, W. Wu, S. Niu, X. Wen, and Z. L. Wang, ACS Nano **7**, 8266 (2013).
[65] J. Yang, J. Chen, Y. Liu, W. Yang, Y. Su, and Z. L. Wang, ACS Nano **8**, 2649 (2014).
[66] U. Khan and S.-W. Kim, ACS Nano **10**, 6429 (2016).
[67] U. Khan, T.-H. Kim, K. H. Lee, J.-H. Lee, H.-J. Yoon, R. Bhatia, I. Sameera, W. Seung, H. Ryu, C. Falconi, and S.-W. Kim, Nano Energy **17**, 356 (2015).
[68] G. Zhu, C. Pan, W. Guo, C.-Y. Chen, Y. Zhou, R. Yu, and Z. L. Wang, Nano Lett. **12**, 4960 (2012).
[69] W. Seung, M. K. Gupta, K. Y. Lee, K.-S. Shin, J.-H. Lee, T. Y. Kim, S. Kim, J. Lin, J. H. Kim, and S.-W. Kim, ACS Nano **9**, 3501 (2015).
[70] S. Wang, L. Lin, and Z. L. Wang, Nano Lett. **12**, 6339 (2012).
[71] S. Kim, M. K. Gupta, K. Y. Lee, A. Sohn, T. Y. Kim, K.-S. Shin, D. Kim, S. K. Kim, K. H. Lee, H.-J. Shin, D.-W. Kim, and S.-W. Kim, Adv. Mater. **26**, 3918 (2014).
[72] G. Zhu, J. Chen, Y. Liu, P. Bai, Y. S. Zhou, Q. Jing, C. Pan, and Z. L. Wang, Nano Lett. **13**, 2282 (2013).
[73] W. Yang, J. Chen, X. Wen, Q. Jing, J. Yang, Y. Su, G. Zhu, W. Wu, and Z. L. Wang, ACS Appl. Mater. Interfaces **6**, 7479 (2014).
[74] Y. Yang, H. Zhang, J. Chen, Q. Jing, Y. S. Zhou, X. Wen, and Z. L. Wang, ACS Nano **7**, 7342 (2013).
[75] B. Meng, W. Tang, Z. Too, X. Zhang, M. Han, W. Liu, and H. Zhang, Energy Environ. Sci. **6**, 3235 (2013).
[76] S. Wang, Y. Xie, S. Niu, L. Lin, and Z. L. Wang, Adv. Mater. **26**, 2818 (2014).
[77] S. Niu, Y. Liu, X. Chen, S. Wang, Y. S. Zhou, L. Lin, Y. Xie, and Z. L. Wang, Nano Energy **12**, 760 (2015).
[78] D. Kim, Y. Oh, B.-W. Hwang, S.-B. Jeon, S.-J. Park, and Y.-K. Choi, ACS Nano **10**, 1017 (2016).
[79] K.-E. Byun, Y. Cho, M. Seol, S. Kim, S.-W. Kim, H.-J. Shin, S. Park, and S. Hwang, ACS Appl. Mater. Interfaces **8**, 18519 (2016).
[80] G. Song, Y. Kim, S. Yu, M.-O. Kim, S.-H. Park, S. M. Cho, D. B. Velusamy, S. H. Cho, K. L. Kim, J. Kim, E. Kim, and C. Park, Chem. Mater. **27**, 4749 (2015).
[81] H. Y. Li, L. Su, S. Y. Kuang, C. F. Pan, G. Zhu, and Z. L. Wang, Adv. Funct. Mater. **25**, 5691 (2015).
[82] C. K. Jeong, K. M. Baek, S. Niu, T. W. Nam, Y. H. Hur, D. Y. Park, G.-T. Hwang, M. Byun, Z. L. Wang, Y. S. Jung, and K. J. Lee, Nano Lett. **14**, 7031 (2014).
[83] W. Yang, J. Chen, G. Zhu, J. Yang, P. Bai, Y. Su, Q. Jing, X. Cao, and Z. L. Wang, ACS Nano **7**, 11317 (2013).
[84] J. H. Lee, R. Hinchet, S. K. Kim, S. Kim, and S.-W. Kim, Energy Environ. Sci. **8**, 3605 (2015).